# A likely universal model of fracture scaling and its consequence for crustal hydromechanics

Philippe Davy, Romain Le Goc, Caroline Darcel, Olivier Bour, Jean-Raynald de Dreuzy, R. Munier

# A likely universal model of fracture scaling and its consequence for crustal hydromechanics

P. Davy,[1] R. Le Goc,[1,2] C. Darcel,[2] O. Bour,[1] J. R. de Dreuzy,[1] and R. Munier[3]

Received 12 October 2009; revised 26 February 2010; accepted 10 May 2010; published 15 October 2010.

[1] We argue that most fracture systems are spatially organized according to two main regimes: a "dilute" regime for the smallest fractures, where they can grow independently of each other, and a "dense" regime for which the density distribution is controlled by the mechanical interactions between fractures. We derive a density distribution for the dense regime by acknowledging that, statistically, fractures do not cross a larger one. This very crude rule, which expresses the inhibiting role of large fractures against smaller ones but not the reverse, actually appears be a very strong control on the eventual fracture density distribution since it results in a self-similar distribution whose exponents and density term are fully determined by the fractal dimension $D$ and a dimensionless parameter $\gamma$ that encompasses the details of fracture correlations and orientations. The range of values for $D$ and $\gamma$ appears to be extremely limited, which makes this model quite universal. This theory is supported by quantitative data on either fault or joint networks. The transition between the dilute and dense regimes occurs at about a few tenths of a kilometer for faults systems and a few meters for joints. This remarkable difference between both processes is likely due to a large-scale control (localization) of the fracture growth for faulting that does not exist for jointing. Finally, we discuss the consequences of this model on the flow properties and show that these networks are in a critical state, with a large number of nodes carrying a large amount of flow.

**Citation:** Davy, P., R. Le Goc, C. Darcel, O. Bour, J. R. de Dreuzy, and R. Munier (2010), A likely universal model of fracture scaling and its consequence for crustal hydromechanics, *J. Geophys. Res.*, *115*, B10411, doi:10.1029/2009JB007043.

## 1. Introduction

[2] Measuring the complexity of fracture networks has been an issue for the last 20 years with consequences on brittle strength, rock permeability, and earthquake dynamics [*Allegre et al.*, 1982; *Crampin*, 1999; *Davy et al.*, 2006; *King*, 1983; *Renshaw*, 1999; *Turcotte*, 1986]. A special focus has been given to the scaling properties of fracture networks that link rock samples to crustal scales (see the pioneer study of *Tchalenko* [1970] and the review paper by *Bonnet et al.* [2001], and references therein). Power laws have been found to likely describe ubiquitously the scaling properties of fracture density with two consequences: (1) Fracture networks are scale-free objects (power law is the only mathematical function that does not require a scale parameter) and (2) long fractures are much more numerous than for any other distribution type (lognormal in particular, which was often taken as the fitting function). Although ubiquitous in natural systems, the reason why this power law scaling emerges is still an issue. It is supposed to derive from a complex, a few say critical, self-organized dynamics, one of whose characteristics is to produce long-range correlated patterns that make large-scale structure probable and "genetically" (thus statistically) linked to smaller ones [*Bak et al.*, 1988; *Bak and Tang*, 1989; *Sornette et al.*, 1990; *Sornette*, 2006].

[3] In this paper, we aim to give a theoretical framework for fracture scaling models based on very basic properties. It is beyond the scope of this paper to discuss how complex forms derive from complex processes; we just acknowledge a few basic properties of fracturing, and we elaborate on the consequences. The points are as follows:

[4] 1. A fracture induces a perturbation of the stress (and strain) field that modify (both enhance and decrease) the occurrence probability for another fracture to initiate and/or grow at its vicinity. The extent of this perturbation is of the order of the fracture length [see, e.g., *Atkinson*, 1987; *Chinnery and Petrak*, 1968; *Segall and Pollard*, 1980] even if longer-range perturbation can be expected when numerous fractures interact [*Herrmann and Roux*, 1990].

[5] 2. For quasi-static fracturing, most of the fracture growth (with the exception of boundary-related fractures) is controlled by the perturbation of stress field induced by the fracture itself and by neighbor fractures [*Atkinson*, 1987]. If

[1] Géosciences Rennes, UMR 6118, CNRS, University of Rennes I, Rennes, France.
[2] Itasca Consultants S. A., Group HCItasca, Ecully, France.
[3] Svensk Kärnbränslehantering AB, Stockholm, Sweden.


0148-0227/10/2009JB007043

the fracture does not produce by itself the reasons for stopping its own growth, it is reasonable to think that the eventual fracture pattern and its scaling law result from a basic property of the fracture-to-fracture mechanical interactions [*Renshaw and Pollard*, 1994; *Segall and Pollard*, 1983; *Segall*, 1984].

[6] We first discuss both end-members of the fracturing process: The dilute case where fractures are likely growing independently from each other and the dense case where fracture growth is fully controlled by the presence of surrounding fractures. We then combine both into a geometrical model of fracture organization that likely applies over the whole range of fracture scales. A key result is that the large-scale part of this model appears to be almost universal; i.e., both the scaling exponents and the density term are, although not strictly fixed, highly constrained and almost independent of the details of the fracturing process, boundary conditions, intensity of fracturing, etc. The relevance of this model can thus be easily checked with actual fracture distribution; we show that it successfully fits the density distribution of fracture networks from meter to tenths of kilometer scales. Finally, we discuss the consequences of the derived organization in terms of fracture connectivity and permeability.

## 2. Fracture Organization Model From Fracture Growth Consideration

### 2.1. Dilute Case

[7] When the density of fracture is low, fractures can freely grow and the eventual size distribution depends on the length dependency of the growth rate function. If the growth rate is a power law:

$$\frac{\mathrm{d}l}{\mathrm{d}t} \sim l^a \tag{1}$$

as it is likely (see *Atkinson* [1987, and references therein] and *Lyakhovsky* [2001, and references therein] for a discussion about rock mechanics), then the fracture density distribution $n(l)$ eventually scales as $n(l) \sim l^{-a}$ if $a \neq 1$, and $n(l) \sim \exp(-l/l_o)$ if $a = 1$ [*Sornette and Davy*, 1991]. Estimating $a$ is an open issue, especially for geological systems. *Lyakhovsky* [2001] reported exponent $a$ (quoted $m/2$ in the article) in the range 1–2.5 from laboratory tests on rock samples and numerical simulations for quasi-static crack growth (actually 1.3–1.8 for the latter), but he mentioned smaller exponents when the growth is controlled by the transport of reactive species to the crack tip and larger ones for large crack lengths. *Sornette and Davy* [1991] argue, from thermodynamic arguments, that the exponent $a$ is likely 2 if the damping force that counterbalances the applied stress does not depend on $l$ and $\mathrm{d}l/\mathrm{d}t$. A few experiments on rock-like materials (dry sand [*Davy et al.*, 1990, 1995; *Sornette et al.*, 1993] and plaster [*Mansfield and Cartwright*, 2001]) and numerical simulations [*Cowie et al.*, 1995; *Hardacre and Cowie*, 2003a, 2003b] also address this issue by analyzing the evolution of quite complex fault network. The power law model was found to correctly fit fracture length distributions even for low-density networks, except for the largest fracture; most of the 2-D exponents (i.e., measured on fault traces) are close to 2.

[8] Note that the growth rate equation (1) includes fracture linkage mechanisms, ubiquitously observed in fracture networks and partly responsible for the displacement-length relationship [e.g., *Cladouhos and Marrett*, 1996; *Cowie and Scholz*, 1992; *Schlagenhauf et al.*, 2008; *Schultz*, 2000; *Schultz and Fossen*, 2002; *Xu et al.*, 2006].

[9] Thus, a general expression of the density length distribution of dilute fracture networks can be

$$n_{\mathrm{dilute}}(l, L) = \alpha l^{-a} L^D \tag{2}$$

where $n_{\mathrm{dilute}}(l, L)\mathrm{d}l$ is the number of fractures in a system of size $L$ (either an area in 2-D or a volume in 3-D) whose length $l'$ is in the range $[l, l + \mathrm{d}l]$. $D$ is formally the mass (or correlation) dimension of the fracture-center network that is smaller or equal to the topological dimension (see *Bonnet et al.* [2001] and *Bour et al.* [2002] for further explanation). As the exponent $a$, $D$ is supposed to be related to some fundamental properties of the fracturing process. The parameter $\alpha$ is the density term that is likely increasing during fracture growth.

[10] Note that the power law distribution is the eventual result of the growth equation (1), which means that it is reached only after a certain time. Before that time, the fracture length distribution is likely dependent on the initial conditions or on the fracture nucleation process.

### 2.2. Dense Case

[11] For dense networks (we will define later how dense they must be), fracture lengths are likely controlled by the fracture-to-fracture mechanical interactions. The cause of limited fracture growth has been widely discussed in the past [*Crampin*, 1994, 1999; *Pollard and Aydin*, 1988; *Renshaw and Pollard*, 1994; *Renshaw*, 1997; *Renshaw et al.*, 2003]. A detailed knowledge of these interactions is hardly measurable and beyond the capacity of numerical models, especially when there is a large number of fractures. Even if the calculation was feasible, it would be difficult to relate the characteristics of the stress field to the eventual fracture distribution. To overcome this difficulty, we develop a very simple model that is based on basic geometrical rules of the fracture-to-fracture interactions for dense networks. By doing this, we aim to capture the fundamental characteristics of network geometry that are consistent with the mechanical interactions.

[12] We first point out that the very basic reason for a fracture to stop growing is to meet another fracture. This assumption is quantitatively supported by the large numbers of T-shape intersections (when a fracture stops on another) compared to X-shape (both fractures cross each other), which makes fracture pattern really different from Poissonian or random equivalents. As an example of this assessment, the number of T-tips per fracture reported on a series of Swedish outcrops (see a detailed description in section 3) ranges from 0.6 to 1.6 with an average of about 1.2, which is by far much larger than any Poissonian realization (for which a T-tip configuration is unlikely).

[13] Second, it makes sense to assume that large fractures inhibit the growth of smaller ones in their vicinity [*Nur*, 1982; *Segall and Pollard*, 1983; *Spyropoulos et al.*, 1999], but that the reverse is not likely to occur. This hierarchical rule is illustrated by *Segall and Pollard* [1983, Figure 11],

and it is basically related to the dependency of both the driving force for fracture growth and the stress perturbation on fracture length [*Griffith*, 1920].

[14] From both these assumptions, we derive a simple statistical rule: A fracture stops growing when it crosses a larger one, which means that the fracture length $l$ is statistically about equal to the distance to the closest larger fracture $d$:

$$l \sim d \tag{3}$$

We now demonstrate that this rule leads to a self-similar distribution of the fracture density distribution. We consider the general case of a fracture network distribution characterized by a density distribution $n(l, L)$, which is the number of fractures of length in the range $[l, l + \mathrm{d}l]$ within a volume (or surface in 2-D) of typical size $L$. The cumulative distribution, $C(l, L) = \int_l^\infty n(l', L)\mathrm{d}l'$, is the number of fractures larger than $l$. If $D$ is the network dimension (which can be a noninteger value for fractal networks), the average distance between the centroids of a fracture of length $l$ and a larger one is [*Bour and Davy*, 1999]

$$d(l) \sim \frac{L}{C(l, L)^{1/D}} \tag{4}$$

Combining equations (3) and (4) yields

$$l = \gamma d = \gamma \frac{L}{C_{\mathrm{dense}}(l, L)^{1/D}} \tag{5}$$

where $C_{\mathrm{dense}}$ is the resulting cumulative distribution and $\gamma$ is a dimensionless ratio, whose order of magnitude is likely close to 1. By deriving equation (4) with $l$, we obtain an expression for the density distribution $n_{\mathrm{dense}}(l, L)$:

$$n_{\mathrm{dense}}(l, L) = D\gamma^D L^D l^{-(D+1)} \tag{6}$$

Note that equation (6) is the only distribution that satisfies the rule (3), and thus both equations (3) and (6) are actually equivalent.

[15] Let us now analyze the property of this distribution. We first notice that it is self-similar since the power law length exponent is exactly the fractal dimension +1 [*Bour et al.*, 2002]. To appraise this geometrical property that qualifies systems whose organization is scale-independent, we try to figure out how the fracture pattern looks like at any scale $L$. For this, we count the number of fractures in a system of size $L$, whose size represents a significant fraction of the system (let us say between $xL$ and $x'L$):

$$N(L) = \int_{xL}^{x'L} n_{\mathrm{dense}}(l', L)\mathrm{d}l' = \gamma^D\left(x^{-D} - x'^{-D}\right) \tag{7}$$

$N(L)$ appears to be independent of $L$, and only dependent on the dimensionless numbers $\gamma$, $x$, and $x'$. An observer who tries to appraise the density of fractures by counting the number of "large" fractures is going to find the same number at all scales. This is the basic property that defines a self-similar pattern.

[16] The second interesting property of this distribution is that its density depends only on two parameters of the initial growing pattern: the correlation dimension $D$ and the geometric parameter $\gamma$.

[17] $D$ is upper bounded by the dimension of the growth space, but can be smaller because of fracture-to-fracture correlations. A collection of fractal dimensions have been measured mainly from 2-D outcrop or lineament maps (see review in the work of *Bonnet et al.* [2001]) with values in 2-D ranging from 1 to 2 and reasonably from 1.7 to 2 (the small values are associated with networks where only a few large fractures are mapped, making the measure somehow meaningless). Little is known about the factors that control $D$ (see, however, *de Arcangelis et al.* [1989], *Hansen et al.* [1991], and *Herrmann and Roux* [1990]). As it measures the fracture-center scaling organization, we expect it to express more the physics of the nucleus phase than of the growth phase. Large-scale localization such as encountered in faulting is the type of correlation that may lower $D$. Note that $D$ is generally measured from the pair correlation function [*Hentschel and Proccacia*, 1983], which is very well defined for large enough networks [*Vicsek*, 1992]. $D$ was found to be smaller for fault networks [*Bour and Davy*, 1999] than for joints [*Bour et al.*, 2002], consistent with the existence of large-scale correlation for the former.

[18] The variable $\gamma$ is expected to vary with fracture orientation distribution. For instance, subparallel fracture sets are supposed to encounter another large fracture at a larger distance than perpendicular fracture sets. We present 2-D simulations that give insight on the range of $\gamma$ values in the next paragraph.

[19] Above all, $\gamma$ encompasses the complexity of fracturing that departs from the simplistic formulated rule (a fracture stops growing when intersecting a larger one), which is basically more probabilistic than absolutely true.

[20] As already mentioned, the distribution is likely universal in the sense that neither $D$ nor $\gamma$ are supposed to vary a lot. We thus call this model likely universal fracture model (UFM), the basic equation (5) being the UFM equation and equation (6) being the UFM distribution.

### 2.3. Transition From Dilute to Dense

[21] We now analyze the transition from dilute to dense network, assuming that they follow equations (2) and (6), respectively. We study the case $a < D + 1$, which is likely in geological systems (see *Bonnet et al.* [2001] and the previous discussion). Note that the reverse case ($a > D + 1$) would end up to a transition from dense to dilute.

[22] We first analyze the distance between a fracture and its larger neighbor in the dilute case. This can be done by using equation (4) with $C(l, L)$ derived from equation (2):

$$d_{\mathrm{dilute}}(l) \sim \left(\frac{a-1}{\alpha}\right)^{\frac{1}{D}} l^{\frac{a-1}{D}}$$

Since $a < D + 1$, the distance increases with $l$ at a rate slower than $l$ (see Figure 1).

[23] It exists a finite length $l_c$ for which $l_c = \gamma d_{\mathrm{dilute}}(l_c)$. For fractures with a length $l < l_c$, the distance between fractures ($d_{\mathrm{dilute}}$) is larger than the fracture length; thus, statistically, fractures are not intersecting their larger neighbor and thus can grow freely according to a growth equation like equation (2). For $l > l_c$, fractures stop growing freely since they are likely crossing a larger one. Their length cannot exceed the distance $d(l)$, and thus they

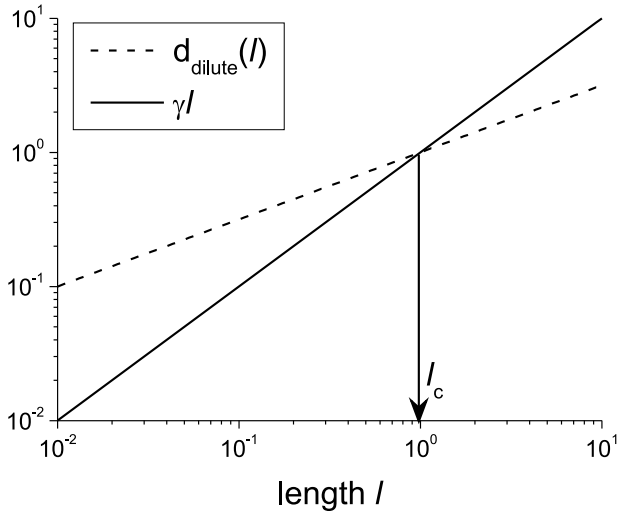


**Figure 1.** Sketch of the evolution of the distance between fractures for each class of fracture length $l$.

obey the UFM length distribution. The transition length is given by

$$l_c = \left(\frac{a-1}{\alpha}\gamma^D\right)^{\frac{1}{D+1-a}} \tag{8}$$

Increasing the density term $\alpha$ leads to a decrease of the fracture-to-fracture distance (and thus to a decrease of $l_c$) and to a larger scale range for the dense regime.

[24] In short, we propose that there is a break in the length distribution scaling due to the transition between a freely growing (dilute) regime and a regime where the fracture-to-fracture interactions are prevailing.

### 2.4. Numerical Simulations

[25] We perform basic numerical simulations with 2-D networks both to check mathematics and to evaluate the $\gamma$ parameter. We assume that the UFM rule (a fracture stops growing when intersecting a larger one) is strictly ensured, which is certainly not true in real systems.

[26] Fractures are first stochastically generated according to a dilute length distribution where $a = 2.3$. Then we remove one by one the shortest top of a fracture that inter sects a larger one. The method is dependent on the order of treating fractures, but we check that this effect does not change the results. The simulations were made with 2-D networks with different orientations and initial distributions. An example of the eventual length distribution is given in Figure 2.

[27] These general principles are validated by numerical simulations and in particular the UFM distribution. For uniformly distributed orientations or two orthogonal sets, $\gamma$ is equal to about 1, giving a density of the UFM distribution $D\gamma^D = 2$. For two fracture sets with an angle of 20°, $\gamma$ is larger, as expected, in the range 1.5–1.7, giving a density term $D\gamma^D$ of 5–6.

[28] Note that this model is neither realistic nor exploited exhaustively (in the sense that we do not explore all possible cases of fracture orientations and intersection rules). However, we do not want to push too far such a "toy" model. We just aim to assess the order of magnitude of $\gamma$ (actually between 1 and 2). Further work is in progress where fractures are nucleating and growing simultaneously according to equation (1) and where the interactions between fractures are much better described (in the same spirit as the work of *Renshaw and Pollard* [1994]).

## 3. Does UFM Applies to Geological Fracture Distribution

[29] We argue that the UFM theory is ubiquitous in natural fracture networks, keeping in mind that the testing of any scaling distribution requires an exhaustive sampling of fracture networks that is barely achieved in geological studies [*Bonnet et al.*, 2001]. We analyze three fracture sets for which we are confident about the data completeness and the mapping method.

[30] Note that the UFM theory has been developed for 3-D networks, but the only data that allow us to test the theory are from 2-D fracture traces. *Darcel et al.* [2003a] demonstrate that if a distribution is self-similar in 3-D, it has the same property in 2-D when cut by a plane and conversely since both the power law length exponents, $a_{2D}$ and $a_{3D}$, and the fractal dimensions, $D_{2D}$ and $D_{3D}$, are linked by the relationship: $X_{2\text{-}D} = X_{3\text{-}D} - 1$, with $X$ either $a$ or $D$. Since the UFM rule ($d$~$l$) is univocally equivalent to a self-similar distribution, a fracture network that is self-similar in 2-D must obey the UFM rule in 3-D. In Appendix A, we give the analytical stereological relationship for the case of randomly oriented disks.

[31] The first data set is the joint network of the Hornelen Basin (Norway) that was mapped carefully at different scales [*Odling*, 1997] and whose scaling properties were thoroughly analyzed in the work of *Bour et al.* [2002]. Seven fracture networks were mapped with outcrop scales ranging from 18 to 720 m. Although the mapping technique was different for small and large outcrops, all the density

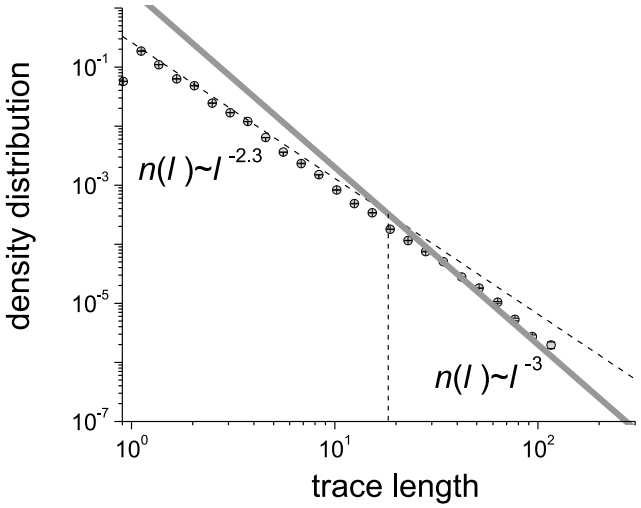


**Figure 2.** Length distribution of a fracture network generated according to the following rules: Fractures are generated using a power law length distribution with an exponent $a = 2.3$ (dashed line), and the eventual distribution results from removing the shortest tip of fractures that intersect a larger one. The bold gray curve is the fit for the large length distribution.

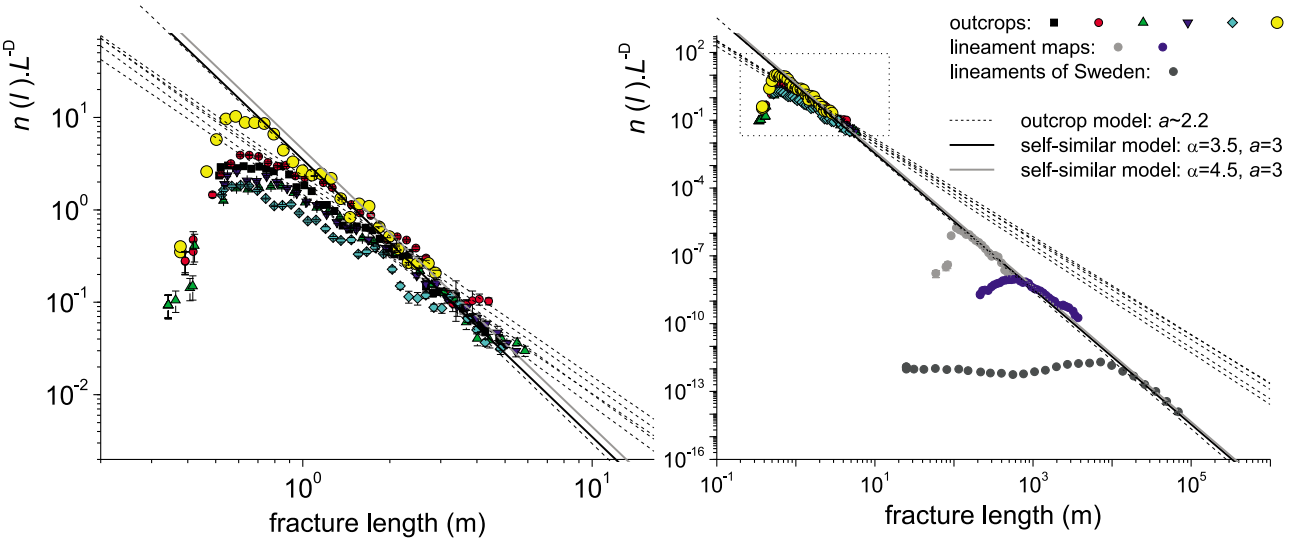


**Figure 3.** (left) Density of fracture length per unit area for both outcrop and lineament maps in Sweden. Outcrops and lineaments are from the Simpevarp and Laxemar areas. The last curve is derived from a compilation of lineaments over Sweden. The dashed lines are power law fits for outcrops. The solid lines are self-similar equations with a density term of 3.5 (black) and 4.5 (gray). (right) The portion of Figure 3 (left) that contains outcrop data.

distributions were found to be consistent with the density equation:

$$n(l, L) = 4.5\ l^{-2.8} L^{1.8} \tag{9}$$

The density term, $\alpha = 4.5 \pm 1$, corresponds to $\gamma = 1.7 \pm 0.2$ according to equation (5). *Odling* [1997] argue that 1 m is a possible physical limit to this power law behavior for this fracture system. No upper limit to this power law scaling was detectable.

[32] The second site series was developed by the Swedish Nuclear Fuel and Waste management company Svensk Kärnbränslehantering AB (SKB) as part of an ongoing investigation conducted to locate a repository for spent nuclear fuel [*Fox et al.*, 2007; *La Pointe et al.*, 2008; *Svensk Kärnbränslehantering AB* (*SKB*), 2004a, 2004b; *Stephens et al.*, 2008; *Wahlgren et al.*, 2008]. The area was deeply investigated with both fracture maps at outcrop scales (0.5–10 m) and regional scales (100–10 km) and a host of deep (~1 km) cored boreholes. At the outcrop scale, fractures are mostly joints and barely faults with a detectable displacement. The large-scale (100–10 km) lineaments that are widespread in the Scandinavian shield are quite heavily fractured shear zones or thick faults with a gouge. The caution with which outcrops have been mapped, with an exhaustive sampling of fractures whose lengths are larger than 50 cm, enables one to give an estimate of the scaling exponent despite the limited range of scales. This was not possible for lineament maps, where an exhaustive detection of fractures and fracture limits is much less reliable. The fracture density distribution is shown in Figure 3. A fit is calculated for each outcrop map (dashed lines in Figure 3) by comparing fracture networks at different scales (bold lines in Figure 3). The exponents measured on outcrops are $a = 2.2$ for all of them except one where a higher density of small fractures is visually detectable (Figure 4). For this latter outcrop, the "through-scale" model is consistent with the fit with the following scaling law:

$$n(l, L) = 4(\pm 1) l^{-3} L^2 \tag{10}$$

The last example is the San Andreas fault map published by *Davy* [1993] from the compilation of *Jennings* [1988]. In terms

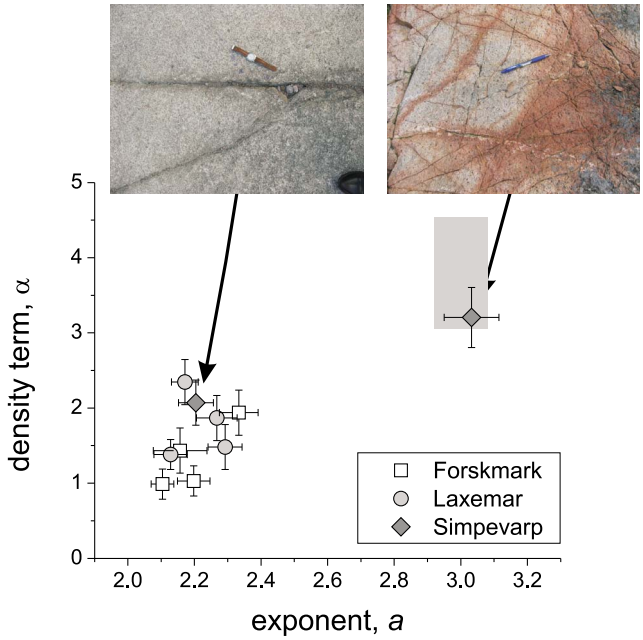


**Figure 4.** Plot of the density term versus the power law length exponent $a$ for all the Swedish outcrops mapped in the Svensk Kärnbränslehantering AB project. The two photographs refer to fracture patterns whose characteristics are indicated. The gray square represents the through-scale model (see section 3).

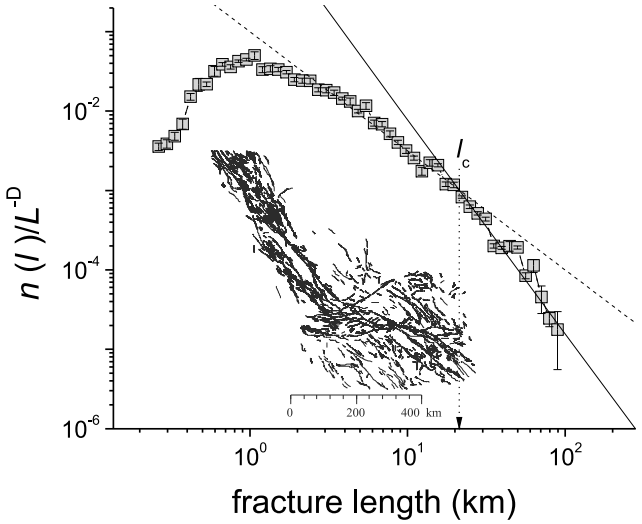


**Figure 5.** The length distribution of the San Andreas fault system from the work of *Davy* [1993] with the fault trace map shown inside the plot. The small-scale dilute distribution (dashed line) has a power law length exponent $a = 1.5$. The large-scale dense distribution is given in the text.

of fracturing mechanisms, we may not expect faulting to be similar to jointing, and we thus expect highly different density distributions. But, expect the differences in orientations, the argument developed in the UFM theory should remain valid and leads to similar conclusions. *Davy* [1993] and *Bour and Davy* [1999] noticed that the length distribution has a power law scaling only for faults smaller than 10 km (Figure 5). The departure from power law for large faults have been interpreted as a segmentation of the largest faults [*Davy*, 1993], or as a truncating effect [*Bour and Davy*, 1999]. The exponent $a$ of the small-scale power law ranges between 1.5 and 2, depending on the correction applied for large fractures. A correlation dimension $D = 1.7$, also smaller than the dimension of joints, has been derived from a correlation analysis. We apply the UFM equation to the density distribution (solid line in Figure 5). The fit is very good for faults larger than 20 km up to the largest recorded fault of 100 km.

[33] The UFM equation obtained for the San Andreas, with $L = 450$ km, is

$$n(l, L) = 4\, l^{-2.7} L^{1.7} \tag{11}$$

All the equations (9), (10), and (11) are consistent with equation (6), with the same density term and $a = D + 1$. They just differ in the fractal dimension $D$.

[34] Finally, we mention that the break in the scaling distribution, which is constitutive of the presented theory, has also been observed on the displacement-length relationship of fractures. On the basis of the analysis of the Krafla fracture swarm (Iceland), which was assumed to be primarily jointing (opening mode) by *Hatton et al.* [1994], *Main et al.* [1999] and *Renshaw and Park* [1997] found a more than linear scaling for fractures smaller than 2.5–70 m and a linear or less than linear scaling for larger fractures. The interpretation of the scaling break is diverse: enhancement of small-fracture aperture by largest one [*Renshaw and Park*, 1997], thermal effects at large-fracture tips [*Hatton et al.*, 1994], or cooperative behavior of large-fracture growth [*Main et al.*, 1999]. The self-similar model, which entails displacement proportional to length, is consistent with the linear relationship observed for large fractures.

## 4. More About Faults and Faulting

[35] The large value of the crossover scale $l_c$ for fault networks (~20 km for the San Andreas system shown in Figure 5) means that most of faults are in the dilute regime. The dense regime may appear rather as an abnormal distribution queue of the dilute regime than as a broad-scaling relationship. This effect was already emphasized on geological networks and experiments. It has been modeled by a gamma or exponential function [*Ackermann et al.*, 2001; *Cowie et al.*, 1994; *Davy*, 1993; *Hardacre and Cowie*, 2003a, 2003b; *Spyropoulos et al.*, 1999] or by a censoring function [*Bour and Davy*, 1999; *Pickering et al.*, 1995]. Apart from the latter, which is a pure statistical effect, the main mechanical causes invoked for this cutoff are the segmentation of large fractures [*Davy*, 1993] or some finite-size effects induced by the thickness of the mechanical layer [*Ackermann et al.*, 2001; *Spyropoulos et al.*, 1999]. In the next paragraph, we discuss the pertinence of the UFM theory and fit relative to processes and data. We illustrate the discussion with the experiments from the work of *Spyropoulos et al.* [1999], *Ackermann et al.* [2001], and *Davy et al.* [1995] and the numerical simulations from the work of *Hardacre and Cowie* [2003b].

[36] In the experiments of *Spyropoulos et al.* [1999] and *Ackermann et al.* [2001], the fracture length distribution evolves toward an exponential function. Cracks are propagating within a brittle layer that is stretched from below by a thick rubber pad. This strong coupling between the brittle layer and the rubber pad controls the eventual spacing between cracks [*Spyropoulos et al.*, 1999]; the brittle thickness is the mechanical length that eventually controls the length distribution. The UFM theory, which postulates that fracture growth is limited by the interaction between fractures, is not appropriate to describe this mechanical system, and thus it cannot predict the dependency on the layer thickness. This is valid for all subparallel joints whose spacing appears to be controlled by a mechanical layer [*Wu and Pollard*, 1995].

[37] The numerical simulations of *Hardacre and Cowie* [2003a, 2003b] seem to end up with similar conclusions: The exponential distribution successfully describes the length distribution of active faults at the later stages, but the boundary conditions are different from those of the aforementioned experiments since the simulations are in 2-D and faults propagate in mode II (i.e., growth is parallel to length). The only characteristic length scale is the system size, which is a limit for fault length rather than a mechanical control. Even if the UFM distribution is a priori not suitable for fitting data, we check how it may explain part of the data shown in in the work of *Hardacre and Cowie* [2003b]. We plot the cumulative UFM:

$$C(l, L) = \int_l^{l_{\max}} n(l', L)\mathrm{d}l' = \int_l^{l_{\max}} D\gamma^D l'^{-D+1} L^D \mathrm{d}l'$$
$$= \gamma^D \left(\frac{l}{L}\right)^{-D} \tag{12}$$

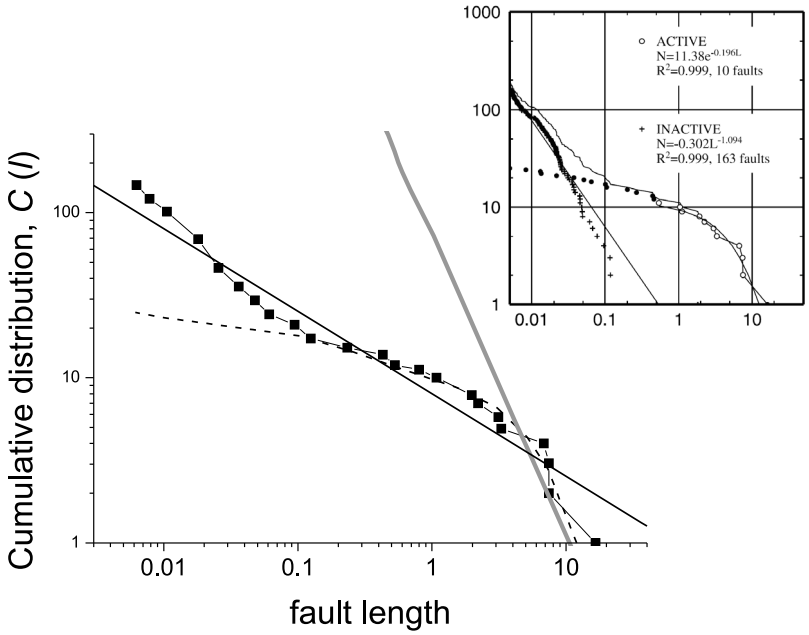


**Figure 6.** Cumulative distribution of faults recorded in the simulation presented in the work of *Hardacre and Cowie* [2003b] (original figure is shown as top right inset). The simulation dimensions are 5 × 10 km. Both active (dashed lines) and total (square points and thin black solid line) faults are shown. The bold gray solid line is the UFM distribution with $L$ = 7 km and $\gamma^D$ = 2.

based on Figure 7 of *Hardacre and Cowie* [2003b], with $\gamma^D$ = 2 and $D$ = 1.8, as found in the previous paragraph for fault networks, and a length $L$ = 7 km, which is the largest fault length (Figure 6). Although any power law exponent cannot be derived from the graph, we find that the UFM equation fits well the distribution extreme at large length. Note, however, that these simulations must be used with caution because (1) faults are not explicitly modeled and the procedure to identify them is quite complex and (2) the number of faults is small (~100), which casts some doubt about the relevance of the large fault distribution.

[38] We do a similar exercise on the experiments from the work of *Davy et al.* [1990, 1995], *Schueller et al.* [2005], and *Sornette et al.* [1993], whose boundary conditions are of the same nature as those used by *Hardacre and Cowie* [2003b]. Again, we find that the UFM distribution fits well the large end-member of the length distribution (Figure 7).

[39] Even if these two examples are successful in demonstrating the validity of the UFM fit at large lengths, we acknowledge that a fit is far from sound scientific proof. We also point out that the scaling information contained in UFM ($l^{-D+1}$) is not actually testable on fault systems because of the very small range of length concerned by the fit. The UFM equation is neither better nor worse than an exponential function, considering the large scattering that is intrinsic to the density of scarce data (Figure 7).

[40] Nevertheless, the UFM equation provides a good fit without any tuning parameter (considering that $D\gamma^D$ = 4 has been obtained for all networks, the fractal dimension can be calculated independently, and $L$ is the system size). In contrast, the exponential fit requires two tuning parameters, one of which is a characteristic length and the other a density. In Figure 7, the exponential fit yields a characteristic length of 3 cm, which is much smaller than $L$ (35–75 cm) and larger than the brittle layer thickness (5 mm).

[41] These considerations give credit to the ability of the UFM theory to describe fault distribution. This is not a

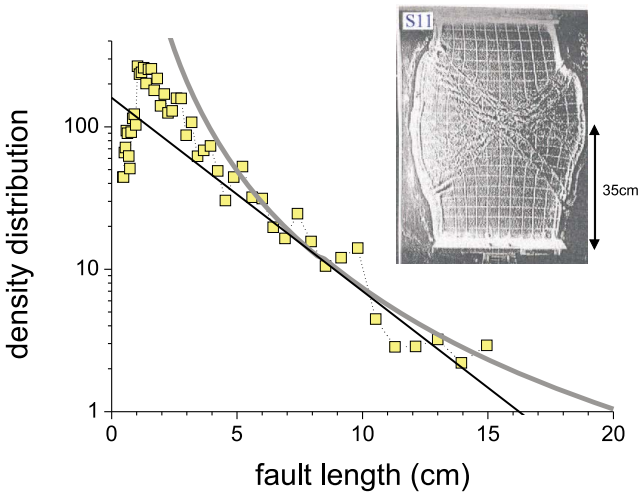


**Figure 7.** The graph represents the density distribution of fault lengths for the last recorded stage (15% of shortening) of the experiment R15 from the work of *Davy et al.* [1995] (yellow squares). The experiment is shown in the top right inset. Its dimensions are 75 × 35 cm. The UFM equation (gray bold solid line) is calculated with $D\gamma^D$ = 4, $D$ = 1.8, and $L$ = 50 mm (the length of the largest fault with an angle of 30° to compression). The exponential fit (black thin solid line) is $n(l) = 160 * \exp(-l/3.2)$.

definite conclusion but definitely an orientation for further work.

## 5. Differences Between Faulting and Jointing

[42] Even if a successful analysis of a few networks is not definite proof, the UFM seems to be a promising theory for both fault and joint networks, although both fracture systems present large differences in terms of processes, density, orientation, and spatial organization. In this section, we discuss further the differences between faulting and jointing.

[43] Note that a precise definition of faulting and jointing can be somewhat ambiguous (see, however, an interesting discussion in the review paper by *Pollard and Aydin* [1988]). Here faulting or jointing refers to the main fracturing process of fracture systems. Faulting or jointing qualifies a fracturing process where most of the fractures exhibit or do not exhibit, respectively, a noticeable shear displacement. Faulting also implies a significant shear displacement at the system boundaries, and large-scale localization is considered to be the eventual stage of faulting.

[44] First, the reason why the UFM theory could be universal partly stays in the simplicity of its basic rule (a fracture stops growing when intersecting a larger one). Nevertheless, the distribution of the joint (Scandinavian outcrops from Norway (Hornelen Basin) and Sweden (Simpevarp, Laxemar)) and fault networks (San Andreas, California) we analyzed present a few significant differences [see also *Bonnet et al.*, 2001]:

[45] 1. $l_c$ is much larger for faults (~20 km) than for joints (1–10 m). A small $l_c$ indicates a higher density in the dilute regime (or a larger density parameter $\alpha$ in equation (2)).

[46] 2. The orientation distribution of faults and joints is quite different. Faults tend to be organized around two orientation poles while the orientation distribution of joints is broader.

[47] 3. The fractal dimension of faults is slightly smaller (1.5–1.8 on 2-D outcrops) than of joints (1.8–2). Even if this difference is not so large, it is significant and emphasizes a higher clustering of faults than of joints. These results highlight the long-range correlations of the faulting process that emerge from the spatial organization of deformation and/or stress [*Davy et al.*, 1990; *Sornette et al.*, 1993]. Note that the density distribution, even if highly quantitative, is quite weak in revealing the details of the fracture organization such as correlation patterns.

[48] How can we explain these factual differences? To our knowledge, this issue is still totally open in the literature. We cannot pretend to have a definite answer; we just point out a few reasons that deserve being tested in further work.

[49] First, the UFM predicts that only a few faults propagate throughout the entire system. This is true both for faults and joints. The fact that $l_c$ for fault systems is close to the system size means that only the largest faults are close enough to interact mechanically. A second observation is that fault networks stop growing when large-scale deformation localization appears [*Hardacre and Cowie*, 2003b; *Sornette et al.*, 1993]. This last stage is concomitant to the development of the largest faults. The fact that $l_c$ remains large even at the eventual stages of the fault development emphasizes a quasi-inhibition of the growth of new small faults after the eventual localization. This is well demonstrated by the numerical simulations of *Hardacre and Cowie* [2003a, 2003b], where both inactive and active faults are analyzed. All these points are relatively well described and justified by experiments, numerical simulations, and theories on faulting.

[50] The case of jointing is more difficult since little is known about it (see, however, *Pollard and Aydin* [1988]). In particular, there is no indication, to our knowledge, about the general evolution of the network growth (whether it eventually stops). The fact that the UFM distribution applies on a very large range of scales indicates (1) that fracture density is limited by the fracture-to-fracture mechanical interactions in a way quantitatively similar to the process that we describe previously and (2) that in contrast to faulting, the dense regime applies to scales much smaller than the system size, meaning that large-scale localization does not stop small-scale fracture growth as it seems to do for faulting. We suspect that this difference between faulting and jointing can be related to the existence of internal stresses in joint systems due to bulk volume changes (thermal expansion/contraction, rock exhumation, etc.), fluid pressure [*Olson*, 1993; *Pollard and Aydin*, 1988], or gravity forces. *Schmittbuhl and Roux* [1994] demonstrated that internal stresses have important consequences on fracture processes and scaling, but they do not calculate explicitly fracture lengths. In particular, *Schmittbuhl and Roux* [1994, p. 50] conclude that "when the internal stresses become larger, the behavior displays a nonvanishing plasticity, as well as a diffuse damage [sic]." This damage and the role played by microcracking is a large difference with faulting and consistent with a high density of microcracks and thus a small value of $l_c$. Apart from this study, there are a few studies that document an increase of the density of small faults, generally because of the coupling with another process, such as ductile materials [*Davy and Cobbold*, 1991; *Davy et al.*, 1995], or dynamic waves [*Poliakov and Herrmann*, 1994].

[51] To conclude, we conjecture that the difference between faulting and jointing is the capacity of small fractures to grow even after the largest fractures appear, and we suspect that this was made possible in joints due to internal stresses.

## 6. Highlighting the Consequences of the UFM Organization

[52] Because the UFM is based on a local condition of fracture connectivity, it likely has important consequences on network connectivity and thus on transport properties (permeability, dispersivity, etc.). The connectivity of fracture networks with a power law length distribution has been studied by *Bour and Davy* [1997, 1998], *Darcel et al.* [2003b], and *Renshaw* [1999]. Large-scale connectivity is ensured both by the presence of large fractures and by the clustering of smaller ones. In $d$ dimensions, connectivity was found to be controlled by the percolation parameter:

$$p = \int_{l_{\min}}^{l_{\max}} \frac{n(l,L)\cdot {l_{\mathrm{inc}}}^{d}}{L^{d}}\,\mathrm{d}l \qquad (13)$$

where $l_{\mathrm{inc}}$ is the part of fracture length that is included in the system of size $L$ [*Bour and Davy*, 1997, 1998] and $l_{\min}$ and

$l_{max}$ are the smallest and largest fracture lengths, which are supposed to be much smaller and larger (respectively) than any characteristic length of the problem. Equation (13) is based on concepts of excluded volume ($l_{inc}^d$) [*Balberg et al.*, 1984; *Huseby et al.*, 1997]; it has been demonstrated to correctly quantify connectivity threshold for 2-D and 3-D networks ($d = 2$ and $d = 3$, respectively). The extension to fractal networks is still an issue: *Berkowitz et al.* [2000] postulated that $d$ can be replaced by the fractal dimension $D$ of network in equation (13), but *Darcel et al.* [2003b] demonstrated from numerical simulations that the resulting expression is not appropriate for 2-D fractal networks. They actually found that equation (13) correctly describes percolation only if $a \leq D + 1$, and if $d$ is the dimension of the embedding space (that is always larger than the fractal dimension $D$). If $a > D + 1$, the connectivity of networks is dominated by the lacunarity of fractal networks, which make infinitely large network always disconnected. Here we consider the former case ($a \leq D + 1$) and assume that expression (13) is valid for 2-D and 3-D fractal networks, with $d$ the dimension of space (either 2 or 3).

[53] Since $l_{inc}$ is $l$ if $l < L$, and $l_{inc} \propto L$ if $l > L$, the integral can be split into both contributions of small and large fractures.

$$p \approx \int_{l_{min}}^{L} \frac{n(l,L)\cdot l^d}{L^d}\mathrm{d}l + \int_{L}^{l_{max}} n(l)\mathrm{d}l$$

In the case $a < D + 1$, which is the likely conditions of the dilute regime, both terms, as well as $p$, are varying as $L^{D+1-a}$ with a few important consequences:

[54] 1. Connectivity increases with the system size $L$. Thus, statistically, small systems are unconnected while large ones are fully connected [*Bour*, 1997; *Bour and Davy*, 1998; *Darcel et al.*, 2003b].

[55] 2. The ratio between both contributions (large and small fractures) is scale-independent.

[56] 3. Because the contribution of large fractures is not negligible, the unconnected-to-connected transition is no more equivalent to a second-order phase transition [*de Dreuzy et al.*, 2001b]. Its width in terms of range of $p$ values does not vanish for very large systems in contrast with the classical percolation theory, where the percolation threshold is equivalent to a second-order phase transition [*Stauffer*, 1979].

[57] The self-similar model with $a = D + 1$, as is the UFM, displays similar property to the classical percolation theory. The percolation parameter is constant (i.e., independent of $L$) [*Darcel et al.*, 2003b] as well as the number of fractures larger than the system size $L$:

$$N(l > L) = \int_{L}^{l_{max}} n(l,L)\mathrm{d}l = \int_{L}^{l_{max}} D\gamma^D l^{-(D+1)} L^D \mathrm{d}l = \gamma^D$$

The likely model for real fracture networks contains both previous cases: $a < D + 1$ for small fractures in the dilute regime and a self-similar distribution for large fractures in the dense regime. We calculate the percolation parameter by taking equation (2) as representative of the dilute regime and equation (6) of the UFM distribution; the transition length between both regimes is $l_c$ defined in equation (8). The percolation parameter writes as the sum of three integrals whose bounds and values depend on the relative position of the crossover scale $l_c$ to system size $L$:

$$P|_{L<l_c} = \int_{l_{min}}^{l_c} \frac{n_{dilute}(l,L)\cdot l^d}{L^d}\mathrm{d}l + \int_{L}^{l_c} n_{dilute}(l,L)\mathrm{d}l + \int_{l_c}^{l_{max}} n_{dense}(l,L)\mathrm{d}l$$

$$P|_{L>l_c} = \int_{l_{min}}^{l_c} \frac{n_{dilute}(l,L)\cdot l^d}{L^d}\mathrm{d}l + \int_{l_c}^{L} \frac{n_{dense}(l,L)\cdot l^d}{L^d}\mathrm{d}l + \int_{L}^{l_{max}} n_{dense}(l,L)\mathrm{d}l$$

By using equations (2), (6), and (8), and assuming $l_{min} \ll L$ and $l_{max} \gg L$, we obtain

$$p|_{L<l_c} = \frac{a-1}{d+1-a}\gamma^D\left(\frac{L}{l_c}\right)^{D+1-a} + \left[\gamma^D\left(\frac{L}{l_c}\right)^{D+1-a} - \gamma^D\left(\frac{L}{l_c}\right)^{D}\right] + \gamma^D\left(\frac{L}{l_c}\right)^{D} = \frac{d\gamma^D}{d+1-a}\left(\frac{L}{l_c}\right)^{D+1-a}$$

$$\text{If } D \neq d, |_{L>l_c} = \frac{a-1}{d+1-a}\gamma^D\left(\frac{L}{l_c}\right)^{D-d} + \frac{D}{d-D}\cdot\gamma^D\left(1-\left(\frac{L}{l_c}\right)^{D-d}\right) + \gamma^D = \frac{d}{d-D}\gamma^D\cdot\left(1-\frac{D+1-a}{d+1-a}\left(\frac{L}{l_c}\right)^{D-d}\right)$$

$$\text{If } D = d, p|_{L>l_c} = \frac{a-1}{d+1-a}\gamma^d + d\gamma^d\ln\left(\frac{L}{l_c}\right) + \gamma^d = d\gamma^d\left(\frac{1}{d+1-a} + \ln\left(\frac{L}{l_c}\right)\right)$$

For systems smaller than $l_c$, the percolation parameter increases with the system size almost as it does for the

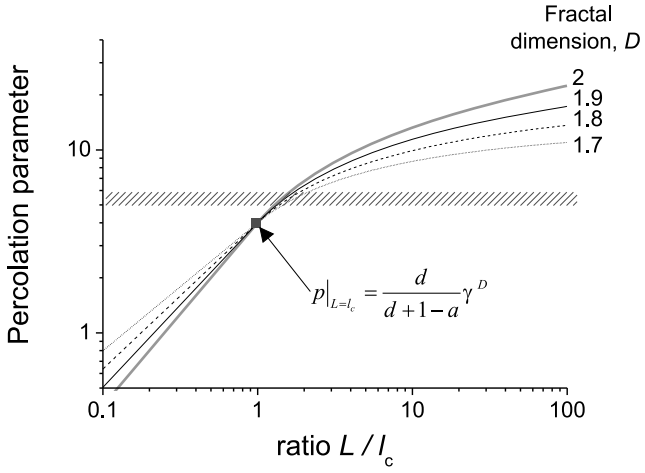


**Figure 8.** Evolution of the percolation parameter with the ratio of $L$ to $l_c$ for different values of the fractal dimension $D$. The exponent $a$ and $d$ are taken equal to 2, as well as $\gamma^D$. The shaded rectangle represents the expected range of percolation threshold.

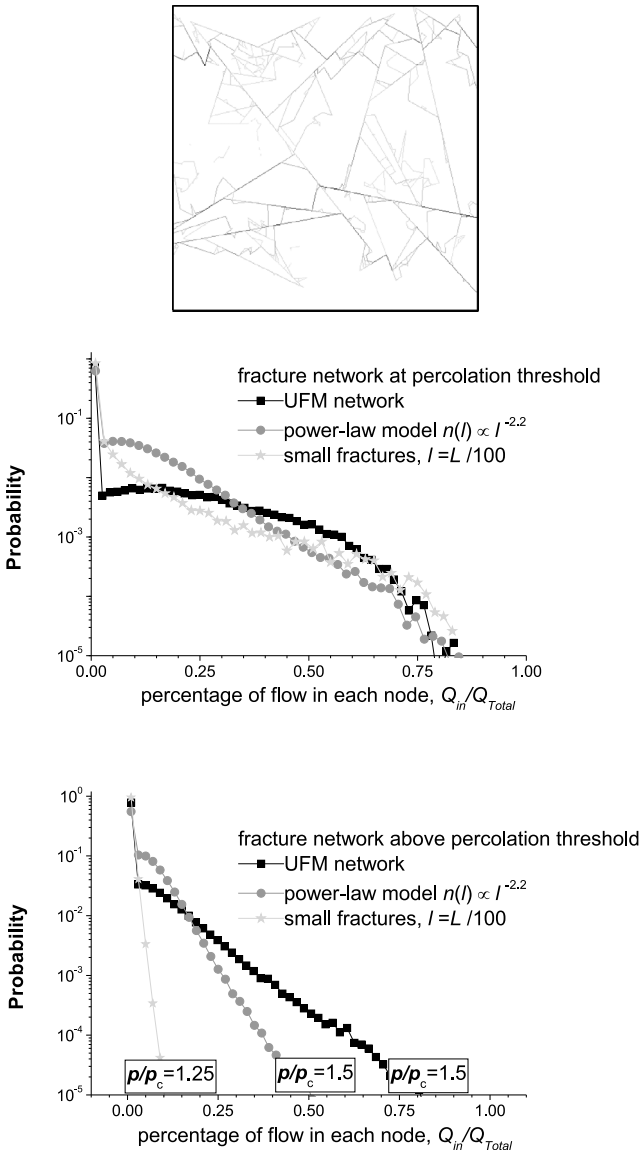


**Figure 9.** (top) A flow pattern of a UFM realization; the frequency distribution of flow at network nodes calculated at (middle) percolation threshold and (bottom) slightly above percolation for $p/p_c$ = 1.25 or 1.5.

simple power law model. At $L = l_c$, the percolation parameter is equal to

$$P|_{L=l_c} = \frac{d}{d+1-a}\gamma^D$$

For larger systems ($L > l_c$), the percolation parameter slightly increases with $L$ as a constant plus an additional term that can be either a slow power law (for $D < d$) or a logarithmic function (for $D = d$). This varying term comes from the contribution of fractures smaller than $L$. The graph in Figure 8 shows the percolation parameter as a function of the ratio $L/l_c$ for 2-D fracture traces with the parameters derived from the analysis of fracture maps presented in the previous paragraph ($\gamma^D \approx 2$, and $d + 1 - a \approx 0.8 - 1$). At $L = l_c$, the percolation parameter is slightly below the percolation threshold in 2-D [*Balberg et al.*, 1984; *Bour and Davy*, 1997; *Robinson*, 1984]. The percolation threshold is reached for $L$ between 1.3 and 2 times $l_c$. Note that $\alpha$, the density term in the dilute regime, is taken into account by $l_c$. This analysis gives a rationale for the intuitive statement that fracture networks are likely below percolation threshold in the dilute regime and above but close to the percolation threshold in the dense regime.

[58] However, the UFM is not only a self-similar model, it also contains spatial correlations between fractures that are likely playing a role on large-scale connectivity and on connectivity changes. Since the UFM is by construction very close to percolation threshold, we expect small change of the fracture position or permeability to have very large consequences on flow.

[59] To illustrate this statement, we calculate flow on the UFM simulations presented in this section. We compare it to two models: small-crack networks, whose behavior is described by the classical percolation theory, and a power law length distribution model with an exponent $a = 2.2$. As a measure of the connectivity organization, we calculate the distribution of incoming flow at the network nodes at percolation threshold and slightly above (Figure 9). The small-fracture case is indicative of what this distribution may look like. At the percolation threshold, there are a large number of nodes carrying a large amount of total flow. Removing these nodes will thus entail large consequences on the flow organization, up to the total disconnection of the system. Above percolation threshold, the flow is much more distributed over nodes; for instance, at $p = 1.25p_c$ (Figure 9, bottom), no node carries more than 10% of total flow.

[60] At percolation threshold, the flow frequency distribution is about similar for the three systems, with a long tail that emphasizes a large number of "critical" nodes (Figure 9, upper graph). Above the threshold, the UFM simulations remain long-tailed, quite similar to the percolation threshold case, while the two other models are much more short-tailed (Figure 9, bottom).

[61] This result highlights how critical the UFM connectivity must be. We may expect small variations to induce dramatic changes of the hydraulic network properties. Let us imagine, for instance, that fractures are ending up very close to their inhibiting neighbor but not intersecting it; the geometric distribution remains about similar to equation (6) but the connectivity will be dramatically reduced. This property puts the emphasis on the detail of fracture intersection (in a mechanistic sense) as a critical control on network permeability. In that respect, the network-connectivity issue is more a concern for mechanical investigations than for classical "percolation-like" network studies.

[62] The connectivity and transport properties of the UFM networks still need more analysis. Further work will be performed on other aspects of connectivity (assortative properties [*Newman*, 2002, 2003], topology, averaging properties [*de Dreuzy et al.*, 2001a; *Desbarats*, 1992], and the role of the intersection length distribution, etc.).

## 7. Conclusion

[63] We argue that most of fracture systems are spatially organized according to two main regimes: a dilute regime for the smallest fractures, where they grow independently of

each other, and a dense regime for which the density distribution is controlled by the mechanical interactions between fractures.

[64] In the dilute regime, the density of fractures increases during the fracturing process, and we do not expect any universality in the density parameter. On the basis of considerations about fracture growth rate and fault trace length measurements, we conjecture that the fracture length distribution could tend to a power law scaling with a 2-D exponent (i.e., measured on fault traces) close to −2.

[65] In the dense regime, we derive the density distribution by acknowledging that, statistically, fractures do not cross a larger one. This simple rule expresses the inhibiting role of large fractures against smaller ones but not the reverse. This very crude description of mechanical interactions actually appears to be a very strong control on the eventual fracture property distribution. Assuming that fracture centers are fractal with a dimension $D$, the only length distribution that satisfies the UFM rule is a power law with an exponent $-(D + 1)$. The fracture density is fully determined by the fractal dimension $D$ and a dimensionless parameter $\gamma$ that encompasses the details of fracture correlations and orientations. The range of values for $\gamma$ appears to be extremely limited, which makes the fracture density distribution quite well constrained. For this reason, we call this model UFM for (likely) universal fracture model.

[66] The smallest fractures are in the dilute regime and the largest fractures are in the dense one. The transition is a length scale $l_c$, which decreases while increasing the density of the dilute regime. This theory is supported by quantitative data on fracture networks. We report three exhaustive studies on fracture distributions for both joint and fault networks for which the UFM successfully provides an excellent fit for the density distributions at large fracture lengths. For smaller fractures, the distribution scaling appears different with smaller power law length exponents, as it is expected for the dilute regime. The transition between this regime and the UFM distribution is about a few tenths of a kilometer for fault systems and a few meters for joints. This is a remarkable difference between both fracture processes whose origin is an open issue. For faulting, the transition length $l_c$ appears to be close to the dimension of the actual mechanical system, meaning that only a few very large faults are in the dense/UFM regime. This is consistent with the almost ending of fault growth (in the dilute regime) once the eventual large-scale localization is achieved. For jointing, we suspect that large-scale localization is no more an inhibiting factor of fracture growth; only the fracture-to-fracture interactions, which are basic to UFM, stop fracture growth. We argue that this difference may be due to the prevailing role of internal stresses in the jointing process. In addition, we point out that the UFM does not apply to fracture systems whose growth is primarily controlled by an external force or constraint.

[67] Since the UFM distribution is well connected by definition, we expect important consequences in the flow properties of fracture network. We calculate the percolation parameter for such a system and demonstrate that it exceeds the percolation threshold once the UFM regime develops. We also give a few insights about the flow organization of fracture networks; in particular, we show that, even above the percolation threshold, the network remains critical with a large number of nodes carrying a large amount of flow.

## Appendix A: Stereology Issue

[68] Let us assume a 3-D density distribution of the form

$$n_{3d}(l, L, \theta, \varphi) = \alpha_{3D}(\theta, \varphi) L^{D_{3d}} l^{-a_{3d}},$$

where $n_{3d}$ $(l, L, \theta, \varphi)\mathrm{d}l\ \mathrm{d}\theta\ \mathrm{d}\varphi$ is the number of fractures of length in the range $[l, l + \mathrm{d}l]$, strike in $[\theta, \theta + \mathrm{d}\theta]$, and dip in $[\varphi, \varphi + \mathrm{d}\varphi]$, within a typical volume of size $L$. If fractures are likely modeled by 2-D disks in a 3-D space, the distribution of 2-D fracture traces is

$$n_{2d}(t, L) = \frac{\sqrt{\pi}}{2} \frac{\Gamma\left(\frac{a_{3d}}{2}\right)}{\Gamma\left(\frac{a_{3d}+1}{2}\right)} \left( \int_0^{\frac{\pi}{2}} \int_0^{\pi} \alpha_{3d}(\theta, \varphi) \sin\varphi \mathrm{d}\theta \mathrm{d}\varphi \right) \cdot L^{D_{3d-1}} t^{-a_{3d}+1},$$

where $\Gamma$ is the gamma function. The density term is thus a complex function of the angular distributions. For uniform orientations, the 2-D density distribution writes as

$$n_{2d}(t, L) = \frac{\alpha}{\sqrt{\pi}} \frac{\Gamma\left(\frac{a_{3d}}{2}\right)}{\Gamma\left(\frac{a_{3d}+1}{2}\right)} L^{D_{3d-1}} t^{-a_{3d}+1},$$

where $\alpha$ is the integral of $\alpha_{3d}$ over strike and dip. This stereological rule, plus the trivial relationship $D_{3d} = D_{2d} + 1$ transforms equation (6) into

$$n_{2d}(t, L) = D_{3d} \gamma^{D_{3d}} \frac{\Gamma\left(\frac{D_{3d}+1}{2}\right)}{\sqrt{\pi}\ \Gamma\left(\frac{D_{3d}+2}{2}\right)} L^{D_{3d}-1} t^{-D_{3d}} \approx 0.4(D_{2d} + 1) \gamma^{D_{2d}+1} L^{D_{2d}} t^{-D_{2d}+1}$$

This equation is not very different from equation (6) written for 2-D fractures. The scaling is similar and the density term is of the same order of magnitude. This emphasizes that the basic geometrical argument that lead to equation (6) (i.e., the fact that a fracture stops on its largest neighbor) is still valid on 2-D traces.

## References


Ackermann, R. V., et al. (2001), The geometric and statistical evolution of normal fault systems: An experimental study of the effects of mechanical layer thickness on scaling laws, *J. Struct. Geol.*, *23*(11), 1803–1819, doi:10.1016/S0191-8141(01)00028-1.

Allegre, C. J., et al. (1982), Scaling rules in rock fracture and possible implications for earthquake prediction, *Nature*, *297*(5861), 47–49, doi:10.1038/297047a0.

Atkinson, B. K. (1987), *Fracture Mechanics of Rock*, 534 pp., Academic, London.

Bak, P., and C. Tang (1989), Earthquakes as a self-organized critical phenomenon, *J. Geophys. Res.*, *94*(B11), 15,635–15,637, doi:10.1029/JB094iB11p15635.

Bak, P., C. Tang, and K. Wiesenfeld (1988), Self-organized criticality, *Phys. Rev. A*, *38*(1), 364–374, doi:10.1103/PhysRevA.38.364.

Balberg, I. C., et al. (1984), Excluded volume and its relation to the onset of percolation, *Phys. Rev. B*, *30*(7), 3933–3943, doi:10.1103/PhysRevB.30.3933.

Berkowitz, B., O. Bour, P. Davy, and N. Odling (2000), Scaling of fracture connectivity in geological formations, *Geophys. Res. Lett.*, *27*(14), 2061–2064, doi:10.1029/1999GL011241.

Bonnet, E., O. Bour, N. E. Odling, P. Davy, I. Main, P. Cowie, and B. Berkowitz (2001), Scaling of fracture systems in geological media, *Rev. Geophys.*, *39*(3), 347–384, doi:10.1029/1999RG000074.

Bour, O. (1997), Transfert de fluides dans les milieux fracturés, Ph.D. thesis, Univ. of Rennes, Rennes, France.

Bour, O., and P. Davy (1997), Connectivity of random fault networks following a power law fault length distribution, *Water Resour. Res.*, *33*(7), 1567–1584, doi:10.1029/96WR00433.

Bour, O., and P. Davy (1998), On the connectivity of three-dimensional fault networks, *Water Resour. Res.*, *34*(10), 2611–2622, doi:10.1029/98WR01861.

Bour, O., and P. Davy (1999), Clustering and size distributions of fault patterns: Theory and measurements, *Geophys. Res. Lett.*, *26*(13), 2001–2004, doi:10.1029/1999GL900419.

Bour, O., P. Davy, C. Darcel, and N. Odling (2002), A statistical scaling model for fracture network geometry, with validation on a multiscale mapping of a joint network (Hornelen Basin, Norway), *J. Geophys. Res.*, *107*(B6), 2113, doi:10.1029/2001JB000176.

Chinnery, M. A., and J. A. Petrak (1968), The dislocation fault model with a variable discontinuity, *Tectonophysics*, *5*(6), 513–529, doi:10.1016/0040-1951(68)90008-5.

Cladouhos, T. T., and R. Marrett (1996), Are fault growth and linkage models consistent with power-law distributions of fault lengths?, *J. Struct. Geol.*, *18*(2–3), 281–293, doi:10.1016/S0191-8141(96)80050-2.

Cowie, P. A., and C. H. Scholz (1992), Growth of faults by accumulation of seismic slip, *J. Geophys. Res.*, *97*(B7), 11,085–11,095, doi:10.1029/92JB00586.

Cowie, P. A., A. Malinverno, W. B. F. Ryan, and M. H. Edwards (1994), Quantitative fault studies on the East Pacific Rise: A comparison of sonar imaging techniques, *J. Geophys. Res.*, *99*, 15,205–15,218, doi:10.1029/94JB00041.

Cowie, P. A., D. Sornette, and C. Vanneste (1995), Multifractal scaling properties of a growing fault population, *Geophys. J. Int.*, *122*, 457–469, doi:10.1111/j.1365-246X.1995.tb07007.x.

Crampin, S. (1994), The fracture criticality of crustal rocks, *Geophys. J. Int.*, *118*(2), 428–438, doi:10.1111/j.1365-246X.1994.tb03974.x.

Crampin, S. (1999), Implications of rock criticality for reservoir characterization, *J. Petrol. Sci. Eng.*, *24*(1), 29–48, doi:10.1016/S0920-4105(99)00021-2.

Darcel, C., O. Bour, and P. Davy (2003a), Stereological analysis of fractal fracture networks, *J. Geophys. Res.*, *108*(B9), 2451, doi:10.1029/2002JB002091.

Darcel, C., O. Bour, P. Davy, and J. R. de Dreuzy (2003b), Connectivity properties of two-dimensional fracture networks with stochastic fractal correlation, *Water Resour. Res.*, *39*(10), 1272, doi:10.1029/2002WR001628.

Davy, P. (1993), On the frequency-length distribution of the San Andreas fault system, *J. Geophys. Res.*, *98*(B7), 12,141–12,151, doi:10.1029/93JB00372.

Davy, P., and P. R. Cobbold (1991), Experiments on shortening of a 4-layer model of the continental lithosphere, *Tectonophysics*, *188*(1–2), 1–25, doi:10.1016/0040-1951(91)90311-F.

Davy, P., et al. (1990), Some consequences of a proposed fractal nature of continental faulting, *Nature*, *348*, 56–58, doi:10.1038/348056a0.

Davy, P., A. Hansen, E. Bonnet, and S.-Z. Zhang (1995), Localization and fault growth in layered brittle-ductile systems: Implications to deformations of the continental lithosphere, *J. Geophys. Res.*, *100*(B4), 6281–6294, doi:10.1029/94JB02983.

Davy, P., O. Bour, J.-R. de Dreuzy, and C. Darcel (2006), Flow in multiscale fractal fracture networks, in *Fractal Analysis for Natural Hazards*, edited by G. Cello and B. D. Malamud, pp. 31–45, Geol. Soc., London.

de Arcangelis, L., et al. (1989), Scaling in fracture, *Phys. Rev. B*, *40*(1), 877–880, doi:10.1103/PhysRevB.40.877.

de Dreuzy, J.-R., et al. (2001a), Hydraulic properties of two-dimensional random fracture networks following a power law length distribution: 2. Permeability of networks based on lognormal distribution of apertures, *Water Resour. Res.*, *37*(8), 2079–2096, doi:10.1029/2001WR900010.

de Dreuzy, J.-R., P. Davy, and O. Bour (2001b), Hydraulic properties of two-dimensional random fracture networks following a power law length distribution: 1. Effective connectivity, *Water Resour. Res.*, *37*(8), 2065–2078, doi:10.1029/2001WR900011.

Desbarats, A. J. (1992), Spatial averaging of hydraulic conductivity in three-dimensional heterogeneous porous media, *Math. Geol.*, *24*(3), 249–267, doi:10.1007/BF00893749.

Fox, A., P. La Pointe, J. Hermanson, and J. Öhman (2007), Statistical geological discrete fracture network model. Forsmark modelling stage 2.2, *Rep. R-07-46*, 271 pp., Sven. Kärnbränslehantering AB, Stockholm.

Griffith, A. A. (1920), The phenomena of rupture and flow in solids, *Philos. Trans. R. Soc. London A*, *221*, 163–198.

Hansen, A., et al. (1991), Scale-invariant disorder in fracture and related breakdown phenomena, *Phys. Rev. B*, *43*(1), 665–678, doi:10.1103/PhysRevB.43.665.

Hardacre, K. M., and P. A. Cowie (2003a), Variability in fault size scaling due to rock strength heterogeneity: A finite element investigation, *J. Struct. Geol.*, *25*(10), 1735–1750, doi:10.1016/S0191-8141(02)00205-5.

Hardacre, K. M., and P. A. Cowie (2003b), Controls on strain localization in a two-dimensional elastoplastic layer: Insights into size-frequency scaling of extensional fault populations, *J. Geophys. Res.*, *108*(B11), 2529, doi:10.1029/2001JB001712.

Hatton, C. G., et al. (1994), Non-universal scaling of fracture length and opening displacement, *Nature*, *367*, 160–162, doi:10.1038/367160a0.

Hentschel, H. G. E., and I. Proccacia (1983), The infinite number of generalised dimensions of fractals and strange attractors, *Physica D*, *8*, 435–444, doi:10.1016/0167-2789(83)90235-X.

Herrmann, H. J., and S. Roux (Eds.) (1990), *Statistical Models for the Fracture of Disordered Media*, 351 pp., North-Holland, Amsterdam.

Huseby, O., et al. (1997), Geometry and topology of fracture systems, *J. Phys. A Math. Gen.*, *30*, 1415–1444, doi:10.1088/0305-4470/30/5/012.

Jennings, C. W. (1988), Fault map of California with locations of volcanoes, thermal springs and thermal wells, 4th ed., Calif. Div. of Mines and Geol, Sacramento.

King, G. (1983), The accommodation of large strains in the upper lithosphere of the earth and other solids by self-similar fault systems: The geometrical origin of b-value, *Pure Appl. Geophys.*, *121*(5–6+), 761–815, doi:10.1007/BF02590182.

La Pointe, P., A. Fox, J. Hermanson, and J. Öhman (2008), Geological discrete fracture network model for the Laxemar site. Site descriptive modelling—Site Laxemar, *Rep. R-08-55*, 260 pp., Sven. Kärnbränslehantering AB, Stockholm.

Lyakhovsky, V. (2001), Scaling of fracture length and distributed damage, *Geophys. J. Int.*, *144*(1), 114–122, doi:10.1046/j.0956-540X.2000.01303.x.

Main, I. G., T. Leonard, O. Papasouliotis, C. G. Hatton, and P. G. Meredith (1999), One slope or two? Detecting statistically significant breaks of slope in geophysical data, with application to fracture scaling relationships, *Geophys. Res. Lett.*, *26*(18), 2801–2804, doi:10.1029/1999GL005372.

Mansfield, C., and J. Cartwright (2001), Fault growth by linkage: Observations and implications from analogue models, *J. Struct. Geol.*, *23*(5), 745–763, doi:10.1016/S0191-8141(00)00134-6.

Newman, M. E. J. (2002), Assortative mixing in networks, *Phys. Rev. Lett.*, *89*(20), 208701, doi:10.1103/PhysRevLett.89.208701.

Newman, M. E. J. (2003), Mixing patterns in networks, *Phys. Rev. E*, *67*(2), 026126, doi:10.1103/PhysRevE.67.026126.

Nur, A. (1982), The origin of tensile fracture lineaments, *J. Struct. Geol.*, *4*(1), 31–40, doi:10.1016/0191-8141(82)90004-9.

Odling, N. E. (1997), Scaling and connectivity of joint systems in sandstones from western Norway, *J. Struct. Geol.*, *19*(10), 1257–1271, doi:10.1016/S0191-8141(97)00041-2.

Olson, J. E. (1993), Joint pattern development: Effects of subcritical crack growth and mechanical crack interaction, *J. Geophys. Res.*, *98*, 12,251–12,265, doi:10.1029/93JB00779.

Pickering, G., et al. (1995), Sampling power-law distributions, *Tectonophysics*, *248*(1–2), 1–20, doi:10.1016/0040-1951(95)00030-Q.

Poliakov, A. N. B., and H. J. Herrmann (1994), Self-organized criticality of plastic shear bands in rocks, *Geophys. Res. Lett.*, *21*(19), 2143–2146, doi:10.1029/94GL02005.

Pollard, D. D., and A. Aydin (1988), Progress in understanding jointing over the past century, *Geol. Soc. Am. Bull.*, *100*(8), 1181–1204, doi:10.1130/0016-7606(1988)100<1181:PIUJOT>2.3.CO;2.

Renshaw, C. E. (1997), Mechanical controls on the spatial density of opening-mode fracture networks, *Geology*, *25*(10), 923–926, doi:10.1130/0091-7613(1997)025<0923:MCOTSD>2.3.CO;2.

Renshaw, C. E. (1999), Connectivity of joint networks with power law length distributions, *Water Resour. Res.*, *35*(9), 2661–2670, doi:10.1029/1999WR900170.

Renshaw, C. E., and D. D. Pollard (1994), Numerical simulation of fracture set formation: A fracture mechanics model consistent with experimental observations, *J. Geophys. Res.*, *99*(B5), 9359–9372, doi:10.1029/94JB00139.

Renshaw, C. E., and J. C. Park (1997), Effect of mechanical interactions on the scaling of fracture length and aperture, *Nature*, *386*, 482–484, doi:10.1038/386482a0.

Renshaw, C. E., T. A. Myse, and S. R. Brown (2003), Role of heterogeneity in elastic properties and layer thickness in the jointing of layered sedimentary rocks, *Geophys. Res. Lett.*, *30*(24), 2295, doi:10.1029/2003GL018489.

Robinson, P. C. (1984), Numerical calculations of critical densities for lines and planes, *J. Phys. A Math. Gen.*, *17*, 2823–2830, doi:10.1088/0305-4470/17/14/025.

Schlagenhauf, A., et al. (2008), Incremental growth of normal faults: Insights from a laser-equipped analog experiment, *Earth Planet. Sci. Lett.*, *273*(3–4), 299–311, doi:10.1016/j.epsl.2008.06.042.

Schmittbuhl, J., and S. Roux (1994), The influence of internal stresses on the fracture of heterogeneous media, *Model. Simul. Mater. Sci. Eng.*, *2*(1), 21–52, doi:10.1088/0965-0393/2/1/003.

Schueller, S., F. Gueydan, and P. Davy (2005), Brittle-ductile coupling: Role of ductile viscosity on brittle fracturing, *Geophys. Res. Lett.*, *32*, L10308, doi:10.1029/2004GL022272.

Schultz, R. A. (2000), Growth of geologic fractures into large-strain populations: Review of nomenclature, subcritical crack growth, and some implications for rock engineering, *Int. J. Rock Mech. Min. Sci.*, *37*(1–2), 403–411, doi:10.1016/S1365-1609(99)00115-X.

Schultz, R. A., and H. Fossen (2002), Displacement-length scaling in three dimensions: The importance of aspect ratio and application to deformation bands, *J. Struct. Geol.*, *24*(9), 1389–1411, doi:10.1016/S0191-8141(01)00146-8.

Segall, P. (1984), Formation and growth of extensional fracture sets, *Geol. Soc. Am. Bull.*, *95*(4), 454–462, doi:10.1130/0016-7606(1984)95<454:FAGOEF>2.0.CO;2.

Segall, P., and D. D. Pollard (1980), Mechanics of discontinuous faults, *J. Geophys. Res.*, *85*, 4337–4350, doi:10.1029/JB085iB08p04337.

Segall, P., and D. D. Pollard (1983), Joint formation in granitic rock of the Sierra Nevada, *Geol. Soc. Am. Bull.*, *94*(5), 563–575, doi:10.1130/0016-7606(1983)94<563:JFIGRO>2.0.CO;2.

Svensk Kärnbränslehantering AB (SKB) (2004a), Preliminary site description. Forsmark area—Version 1.1, *SKB Rep. R-04-15*, Stockholm.

Svensk Kärnbränslehantering AB (SKB) (2004b), Preliminary site description. Simpevarp area—Version 1.1, *SKB Rep. R-04-74*, Stockholm.

Sornette, D. (2006), *Critical Phenomena in Natural Sciences Chaos, Fractals, Selforganization and Disorder: Concepts and Tools*, 2nd ed., 528 pp., Springer, Heidelberg.

Sornette, D., and P. Davy (1991), Fault growth model and the universal fault length distribution, *Geophys. Res. Lett.*, *18*(6), 1079–1081, doi:10.1029/91GL01054.

Sornette, D., P. Davy, and A. Sornette (1990), Structuration of the lithosphere in plate tectonics as a self-organized critical phenomenon, *J. Geophys. Res.*, *95*(B11), 17,353–17,361, doi:10.1029/JB095iB11p17353.

Sornette, A., P. Davy, and D. Sornette (1993), Fault growth in brittle-ductile experiments and the mechanics of continental collisions, *J. Geophys. Res.*, *98*(B7), 12,111–12,139, doi:10.1029/92JB01740.

Spyropoulos, C., W. J. Griffith, C. H. Scholz, and B. E. Shaw (1999), Experimental evidence for different strain regimes of crack populations in a clay model, *Geophys. Res. Lett.*, *26*(8), 1081–1084, doi:10.1029/1999GL900175.

Stauffer, D. (1979), Scaling theory of percolation clusters, *Phys. Rep.*, *54*(1), 1–74, doi:10.1016/0370-1573(79)90060-7.

Stephens, M. B., et al. (2008), Geology Forsmark. Site descriptive modelling Forsmark stage 2.2, *Rep. R-07-45*, 224 pp., Sven. Kärnbränslehantering AB, Stockholm.

Tchalenko, J. S. (1970), Similarities between shear zones of different magnitudes, *Geol. Soc. Am. Bull.*, *81*(6), 1625–1640, doi:10.1130/0016-7606(1970)81[1625:SBSZOD]2.0.CO;2.

Turcotte, D. L. (1986), A fractal model for crustal deformation, *Tectonophysics*, *132*, 261–269, doi:10.1016/0040-1951(86)90036-3.

Vicsek, T. (1992), *Fractal Growth Phenomena*, 488 pp., World Sci, London.

Wahlgren, C.-H., et al. (2008), Geology Laxemar. Site descriptive modelling SDM—Site Laxemar, *Rep. R-08-54, Sven.*, Kärnbränslehantering AB, Stockholm.

Wu, H., and D. D. Pollard (1995), An experimental study of the relationship between joint spacing and layer thickness, *J. Struct. Geol.*, *17*(6), 887–905, doi:10.1016/0191-8141(94)00099-L.

Xu, S. S., et al. (2006), Effect of sampling and linkage on fault length and length–displacement relationship, *Int. J. Earth Sci.*, *95*(5), 841–853, doi:10.1007/s00531-005-0065-3.

O. Bour, P. Davy, J. R. de Dreuzy, and R. Le Goc, Géosciences Rennes, UMR 6118, CNRS, University of Rennes I, Campus de Beaulieu, F-35042 Rennes CEDEX, France. (philippe.davy@univ-rennes1.fr)

C. Darcel, Itasca Consultants S. A., Group HCItasca, 64 Chemin des Mouilles, F-69130 Ecully, France.

R. Munier, Svensk Kärnbränslehantering AB, Box 5864, SE-102 40 Stockholm, Sweden.